Materials Research Proceedings 41 (2024) 832-841 https://doi.org/10.21741/9781644903131-91

Design of an experimental simulator of void closure during hot rolling process

GOPAKUMAR Akhil[1,2,a *], LANGLOIS Laurent[2,b], PONDAVEN Corentin[1,c] and BIGOT Régis[2,d]

[1]ABS Centre Métallurgique, 10 rue Pierre Simon de Laplace 57070 Metz, France

[2]Laboratoire de conception fabrication Commande (EA 4495), Arts et Métiers Institute of Technology, Université de Lorraine, HESAM université, 4 rue Augustin Fresnel 57070 Metz, France

[a]a.gopakumar@absacciai.com, [b]laurent.langlois@ensam.eu, [c]c.pondaven@absacciai.com, [d]regis.bigot@ensam.eu

Keywords: Open Die Forging, Experimental Simulation, Finite Element Simulation, Porosity Closure

Abstract. The shrinkage porosities produced during the casting of steel blooms has to be fixed by the subsequent hot rolling process. To design the rolling route, finite element simulations integrating void closure models are necessary. However, these models have to be validated by experimental results. Because experiments under industrial conditions are hardly achievable, experimental simulations at lower scale can be considered. However, the experiment must be designed so as to reproduce industrial like conditions concerning the thermomechanical loading and microstructure with respect to void closure. Among the main parameters driving void closure are the equivalent plastic strain and the mean triaxiality. This paper is dedicated to the design of an experimental simulator of void closure during hot rolling. The simulator consists of several strokes performed on a sample containing a real shrinkage porosity, between shaped anvils and with alternations of the forming direction.

Introduction

Hot rolling process is employed after the casting of blooms to have the proper metallurgical properties for the desired application. Moreover, during the rolling process the closure of shrinkage porosities is aimed. The study of the void closure can be substantial in optimizing the rolling process and increasing the efficiency of the process. The void closure has two stages, geometric closure and healing, as highlighted by Park and Young [1]. In the present study, only the geometric closure is considered. The parameters that govern void closure are the thermomechanical loading parameters and the geometry of the pore. The thermomechanical loadings concern mainly the plastic strain, the stress triaxiality with a fundamental effect of the change in the loading direction. The influential geometric parameters of the pore are its global shape (sphere, ellipsoid…) and its tortuosity corresponding to the local irregularities. To study the evolution of the void, the numerical simulation is commonly used integrating full field or mean field models as in Saby's [2] or Pondaven *et al.* [3] works. The full-field model considers an explicit pore to accurately predict its closure. This approach has limitations concerning the number of pores than can be considered and the high computation time. The mean field is used to bypass these limitations as it uses analytical or phenomenological formulation describing geometrical parameter fields such as the volume or the aspect ratio of the pores whose evolutions are governed by equation involving the thermomechanical loading parameters, mainly the equivalent plastic strain and the stress triaxiality. The pores are thus considered through parameter fields characterizing their geometry. The Cicaporo 2 model is a mean-field model developed by Saby *et al*. [4] that was identified using

a numerical design of experiments performed with a full-field model. This model has limitations when applied to multi-stroke forming processes with alternations of loading direction. The model was later modified by Hibbe *et al.* [5] to overcome this limit and validated for ellipsoidal pores. Nevertheless, the current mean field models do not consider a description of the 'tortuosity' of the pore in their formulation which can lead to inadequate prediction of closure.
New approaches involving additional parameters characterizing the tortuosity or based on data learning method can be considered. These approaches need numerical design of experiments with a full-field model able to consider the fine geometrical details of the pores. Such models have to be validated by comparison with experiments for real 'tortuous' pores and thermomechanical paths including change of the loading direction. The actual paper presents the development of an experimental simulator of shrinkage porosity closure during multi-stroke hot forming process with alternations of the forming direction. This simulator consists in forging radially, between V and flat dies, a cylindrical billet containing a real shrinkage porosity. V shape anvils are chosen accordingly to their ability to apply quite a large range of triaxiality and strain [6],[7] representative of cogging or rolling processes.

The next part of the article is dedicated to the experimental simulator design. A second part is devoted to the design of forming routes for the study of void closure during hot rolling. Finally, a first application with drilled samples is presented to show the ability of the simulator to capture the effect of a change of the loading direction.

Design of the Experimental Device

The experimental device, shown in Fig.1, consists of successive strokes performed between V-shaped and flat anvils to apply the triaxiality and equivalent strain ranges representative of an industrial hot rolling process. The sample implemented in the experimental simulator is a cylindrical billet containing a real naturally generated shrinkage porosity as in Pondaven *et al.* [3]. The zone of the sample containing the pore undergoes radial compression. Between two successive strokes, the sample, handled by a gripper mounted on a 6-axes robot, is rotated of 90° to reproduce the typical alternation of the forming direction of hot rolling.

The initial position and orientation of the pores within the sample is determined by X-Ray tomography control. One of the main challenges is the mastering of the position and orientation of the pore through the complete forming route. During the strokes, the sample undergoes elongation with respect to its axis and transverse widening. The gripper must accommodate the deformation of the sample during the stroke, but the system must be able to calculate the theoretical position of the porosity after deformation to reposition the sample before the following stroke. To do that, the displacement of both faces of the billet is measured using a laser system on the free side of the sample and by the gripper system itself on the robot side. The total elongation and the corresponding theoretical position of the pore in the sample are then calculated. This last calculation is performed directly by the robot controller for the achievement of the route to be completely automatized.

The pore closure is followed through X-ray tomography at different stages of the forging route. The initial diameter of the sample is fixed to 30 mm achieving a compromise between the X-Ray tomography capability and the minimum admissible ratio between the diameter of the pore and the diameter of the sample. A maximum void to billet ratio of 1/10 is recommended to reduce the disturbance of the macroscopic thermomechanical fields by the presence of the pore as used by Feng et Cui [8] (void to billet ratio of 0.07) to confront numerical full field and mean field model with experiment results. The next part is devoted to the anvil design.

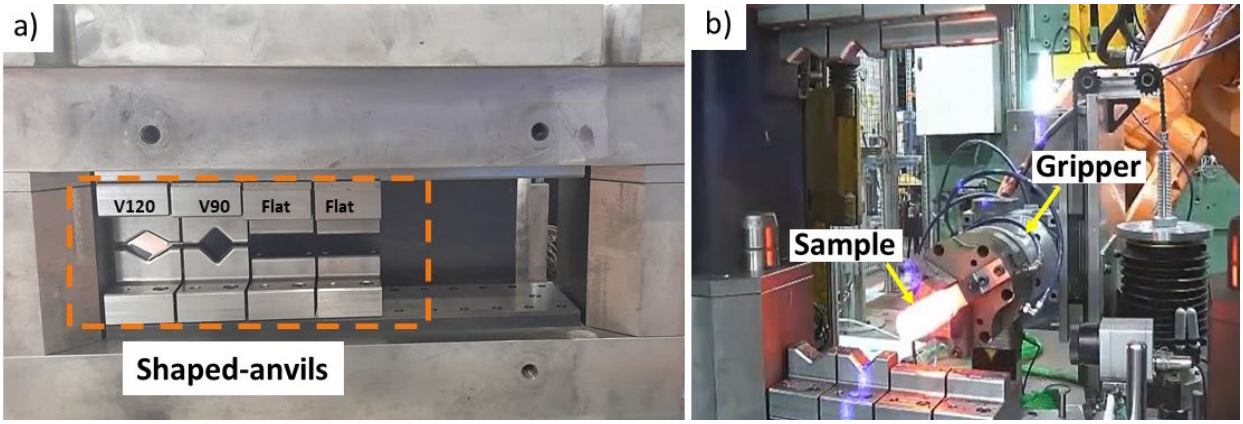

Fig.1 Experimental device, a) Set of V-Shaped anvils, b) The complete device with the instrumented gripper.

Anvil design validation.

The first step is to find the required anvil dimensions to ensure that the proper thermomechanical properties are achieved at the centre of the sample during forging. The design profile of the die is shown in Fig.2. Using this profile, a parametrized 3D CAD model of the dies is constructed. The anvil width W_a and depth, H, need to be optimized to have the proper distribution of the equivalent strain and stress triaxiality. The entry and exit radius are fixed at 2 mm. L_f is taken as zero and α = 60° for V120, 45° for V90 and 0° for flat die. To determine the depth, H, and width, W_a, design criteria are defined.

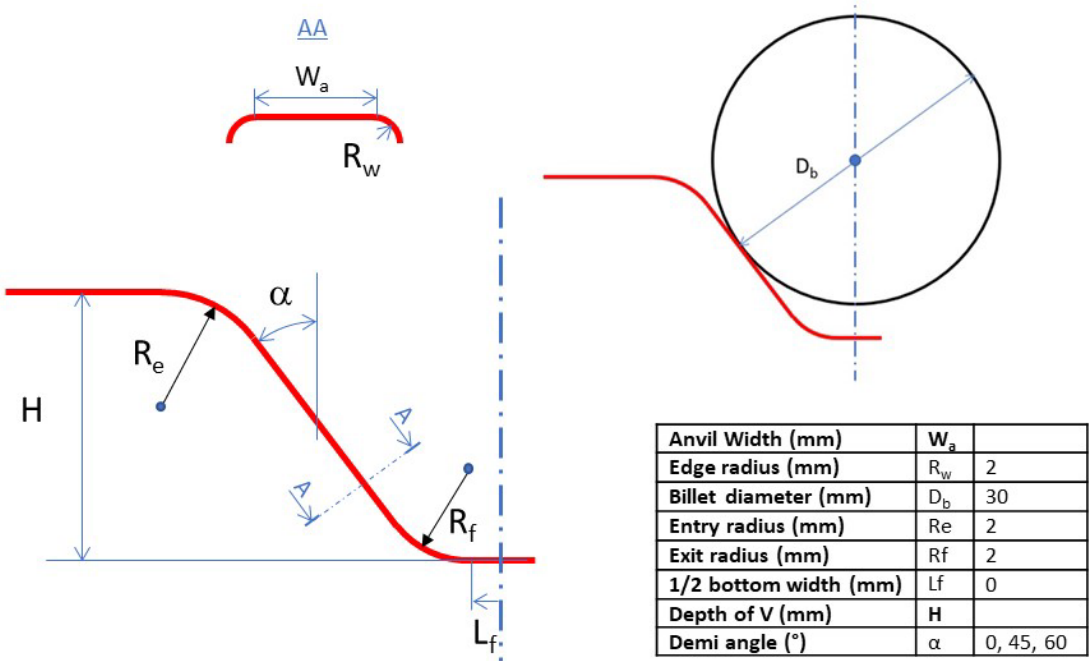

Anvil Width (mm)	W_a	
Edge radius (mm)	R_w	2
Billet diameter (mm)	D_b	30
Entry radius (mm)	Re	2
Exit radius (mm)	Rf	2
1/2 bottom width (mm)	Lf	0
Depth of V (mm)	H	
Demi angle (°)	α	0, 45, 60

Fig.2 General profile of the V dies used to design the anvils.

Criteria for the design of anvils.
The aimed equivalent plastic strain and stress triaxiality must be achieved before the lower and upper anvils get into contact with each other and without the formation of flash (see Fig.3.a). The second criterion concerns the homogeneity of the thermomechanical fields (equivalent strain and stress triaxiality) in the deformed zone. The size of this zone must be large enough compared to the volume of the pore (Fig.3.b) and to ensure a greater tolerance with respect to the pore position offset inevitably introduced by the experimental set-up (Fig.3.c). The homogeneity is linked to the anvil width where larger width increases the axial length of the homogenous zone. Therefore, an optimization of the anvil width is necessary, since the anvil width is likely to influence the applied thermomechanical fields and particularly the repartition between the elongation and the widening of the sample during its forming.

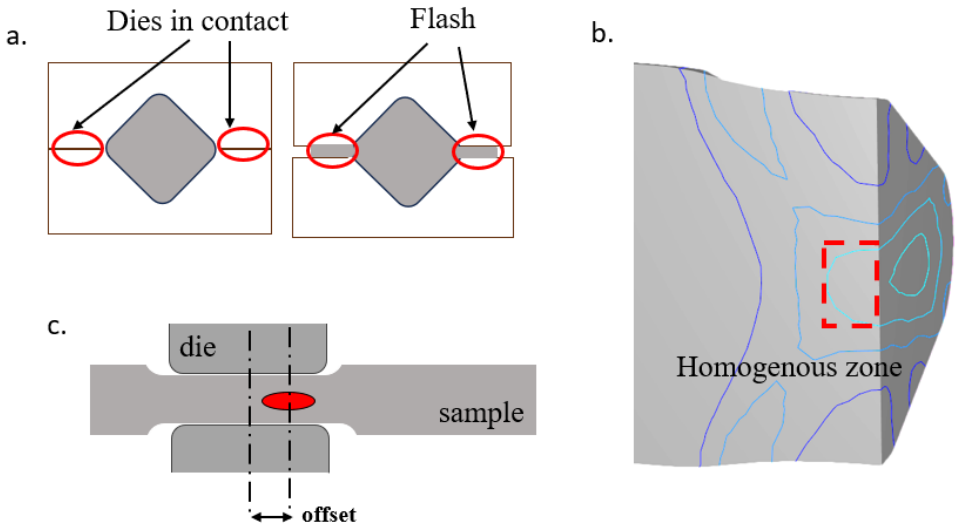

Fig.3 a) Contact between dies before reaching the aimed deformation and flash formation at the end of the forming b) Homogeneity of thermomechanical parameters (equivalent strain) c) Tolerance to the positioning of pore using robot.

The different criteria are checked by FE simulation performed using Forge®NxT4.0. For the first two criteria, a conventional FE model is sufficient while the third criterion is validated using the full-field model developed in the next section.

Full-field numerical modelling of the experimental simulator.
A simulation model with a spherical pore of diameter 3 mm was used to model the forging of a sample using the designed anvils. The first two criteria, validated by conventional FE simulations, have led to an anvil width of 30 mm. Here, the material taken as reference is the 25MnCrS4 steel, corresponding experimentally to that of the container where the pore was inserted in [3]. It can be noted that the designed set of anvils should be applicable for any other low alloyed steel grades.

The full-field simulation is performed to ensure that the sample positioning variability introduced by the robot gripper does not significantly modify the void closure evolution. Mesh boxes were assigned to mesh the billet as shown in the figure 4. The mesh size is set up to 0.0625 mm in the vicinity of the pore and 1 mm far from it. To ensure a regular progression of the mesh size, four concentric mesh boxes are implemented. The mesh sizes in the different boxes are given in Fig.4. The sample free extremity is at a distance of 30 mm from the center of the tools (Fig.4) same as that of the experiment set up.

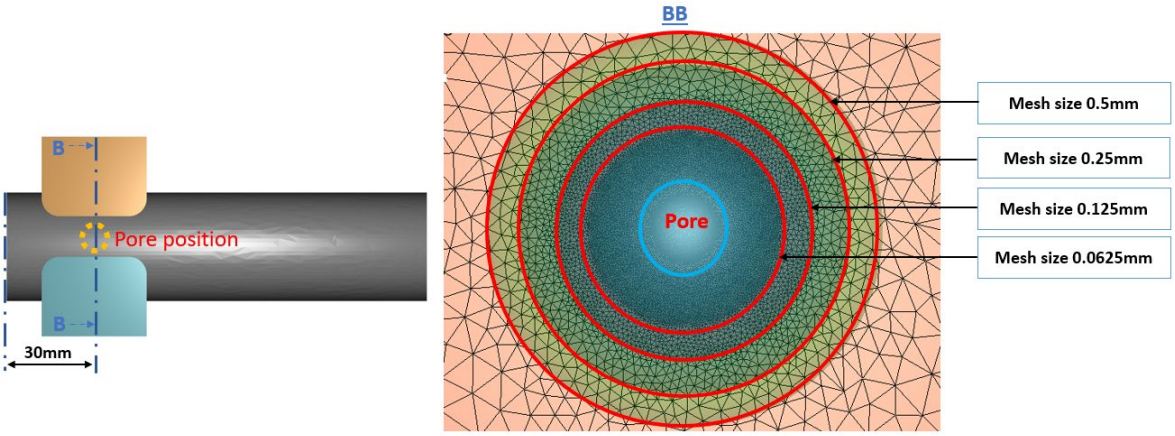

Fig.4 Mesh around the pore using mesh boxes.

The flow stress σ0 is modelled using the Hansel-Spittel law (Equation 1) where ε, $\dot{\varepsilon}$ and T are the equivalent plastic strain, the equivalent plastic strain rate and the temperature respectively.

$$\sigma_0 = A_1 e^{m_1 T} \varepsilon^{m_2 T} \dot{\varepsilon}^{m_3 T} e^{\frac{m_4}{\varepsilon}} \quad (1)$$

The material coefficients given in the table 2 are taken from [3].

Table 1 Hansel-Spittel coefficients 25MnCrS4.

A_1	m_1	m_2	m_3	m_4
1 321.900	-0.002 570	-0.194 100	0.146 800	-0.065 210

The friction between the anvils and billet is modelled using the Tresca limited Coulomb law and the thermal interaction between the dies and the billet is modelled in the simulation to calculate the temperature of the billet during the forging process. The coefficients are shown in table 3 [3].

Table 2 Friction and thermal exchange modelling coefficients.

Coulomb μ	Tresca m	Emissivity	Thermal exchange environment ($W.m^{-2}. K^{-1}$	Thermal exchange anvils ($W.m^{-2}. K^{-1}$)
0.4	0.8	0.88	10	2 000

The billet along with the pore is forged at 1 200 °C. The pore after forging is extracted from the billet mesh using GOM® Inspect 2019 software, and the dimensions and shape factors are calculated using python script (numpy-stl) to post-process the billet mesh after the forming simulation. The remeshing megamaf (function of Forge®NxT4.0) is used to suppress the remeshing when the internal self-contact of the pores is occurring. To observe the impact of the offset, centered and shifted pores with an offset of 0.7 and 1 mm are compared after forging, both cases to a final gap between the upper and lower anvil top surface of 3.7 mm.

In the Fig.5, the cross-section of the pores after forging for the two cases of offset is compared using GOM® Inspect 2019. Here, the maximum deviation is found to be 0.08 mm and 0.04 mm for 1 mm and 0.7 mm offset respectively. The positioning accuracy of the experimental set-up being about 0.5 mm the anvil width of 30 mm is validated.

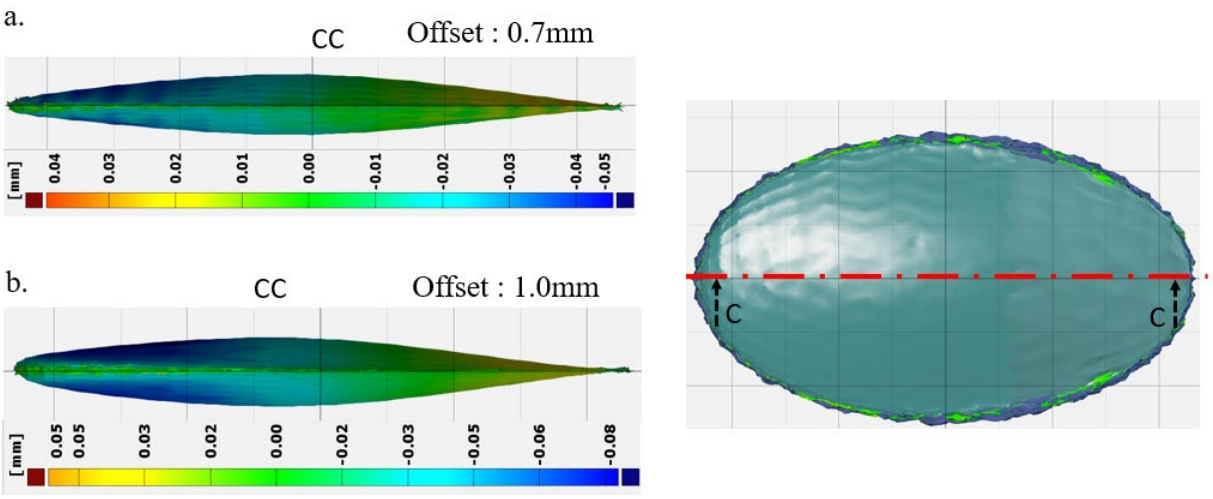

Fig.5 a) Comparison of pore between centered pore and pore at an offset of a) 0.7 mm and b) 1 mm.

The next section is dedicated to the design of different forming routes to study the effect of the change in the deformation direction on void closure.

Design of Forging Route

Using the validated V and flat anvils, forging routes need to be proposed by analysing the equivalent strain and triaxiality for each stroke. To fix the gaps for each stroke, the equivalent strain, $\varepsilon_{reference}$, determined by the FE simulation of the industrial rolling process is considered as a reference [9]. The proposed route is shown in Fig.6.

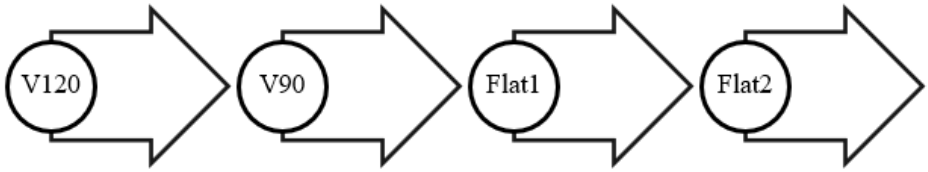

Strokes	V120	V90	Flat1	Flat2
$\varepsilon_{reference}$	0.3	0.2	0.14	0.45

Fig.6 The proposed route with the aimed reference equivalent plastic strain of each stroke.

The proposed methodology consists in analyzing the stress triaxiality and the mean stress triaxiality with respect to the equivalent strain at the center of the deformed zone of the sample. The driving parameter of a stroke is the final gap between the upper and the lower anvils. A route is thus defined by a set of four gaps, one per stroke. To determine the selected gaps, each stroke is simulated until the equivalent strain at the center of the sample reaches its reference value (Fig.6). The billet obtained at the end of a stroke is used for the simulation of the following stroke after a rotation of 90° to alternate of the forming direction.

The simulated evolution of the stress triaxiality and mean stress triaxiality during the first stroke of the first route is shown in Fig.7.

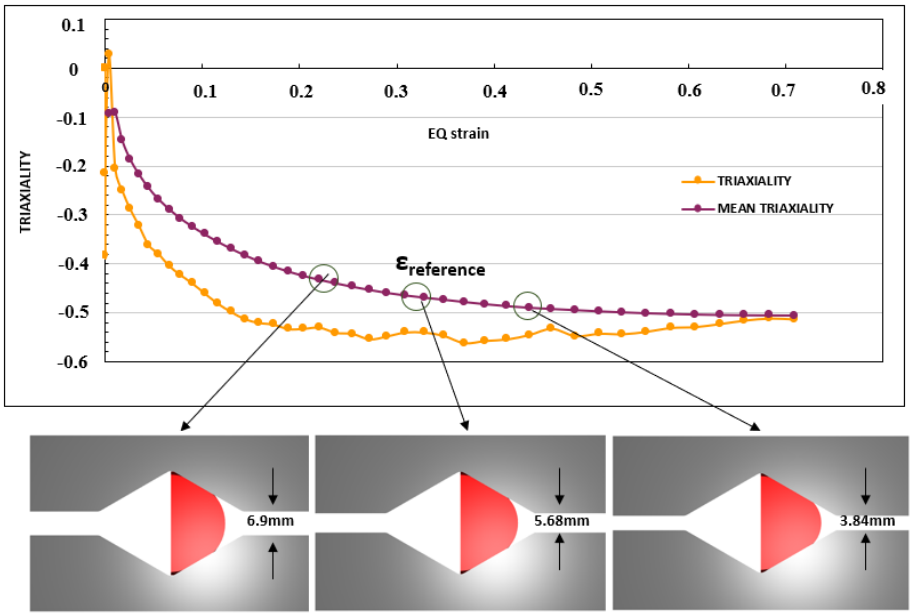

Fig.7 Triaxiality vs equivalent strain for the first stroke(V120) for route 1 with cross-section extraction for three different final gaps.

A gap of 5.7 mm is needed to obtain at the center of the sample the aimed equivalent strain ($\varepsilon_{reference}$). For V120 the stress triaxiality value becomes nearly constant from a strain of 0.2 (figure 7). The strain ranges from 0.2-0.45 provides a constant stress triaxiality. Using the deformed billet for a gap of 4 mm the second stroke is done after rotating the deformed billet at 90°. Then the process continues till the end of the forging routes. The cumulated strain is calculated by summing the strains achieved individually by each stroke that is 1.51 for the studied route.

By modifying the gaps of the route, it is possible to apply different levels of equivalent plastic strain under quite constant stress triaxiality. The designed anvils also allow the application of different routes. These degrees of freedom are useful for the study of the influence of the thermomechanical loading on void closure.

Results and Discussion.

The forming test is conducted for samples made of 41Cr4. The material selected is different from that used for the design of the anvils for a first validation of the extension of the forging test to other low alloyed steel grades. To observe pore closure, billets with a drilled hole of 3.2 mm diameter and 47 mm length are used. The billets are forged according to first two strokes of the forming route of figure 6. The robot-gripper system is used to position the billet on the tool and rotates the sample by 90° for each forging stage. The trials are run multiple times to check the repeatability of the test. The samples are heated to 1,200°C in an electric furnace and placed into the gripper manually after the removal of the oxide scales. No lubrication is applied on the anvils and the samples are air-cooled after forging. The samples are then sand blasted and 3D-scanned for comparison with the FE results. The samples are finally cut for the cross-section observation of the drilled hole evolution after forging.

In parallel, the numerical simulation of the forging test is performed with Forge®NxT4.0 according to the full field modelling procedures described in section 2.3 (except for the Hansel-Spittel law) with a sample (41Cr4) containing a cylindrical hole instead of a sphere. The applied time cycle of the simulation corresponds to that individually measured during each trial. Concerning the material behaviour, the simulation are performed are performed using the Hansel-

Spittel parameters of 41Cr4 from the Forge®NxT4.0 database using the coefficients given in table 3.

Table 3 Hansel-Spittel coefficients 41Cr4 (Forge®NxT4.0 database).

A_1	m_1	m_2	m_3	m_4
1 620.466	-0.002 770	-0.174 240	0.154 100	-0.064 970

The global analysis of the 3D-scan geometry of the sample highlights a slight bending in the deformed zone of the sample (illustrated in Fig.8). The geometry of the section in the deformed zone is not centered on the axis of the not deformed cylindrical zone of the sample. This dissymmetry can come from a difference in friction between the upper and the lower dies or a parallelism defect between the initial sample axis and that of the V anvils. It can be noted that this defect is not constant from one trial to the other and is a source of non-repeatability of the experiments.

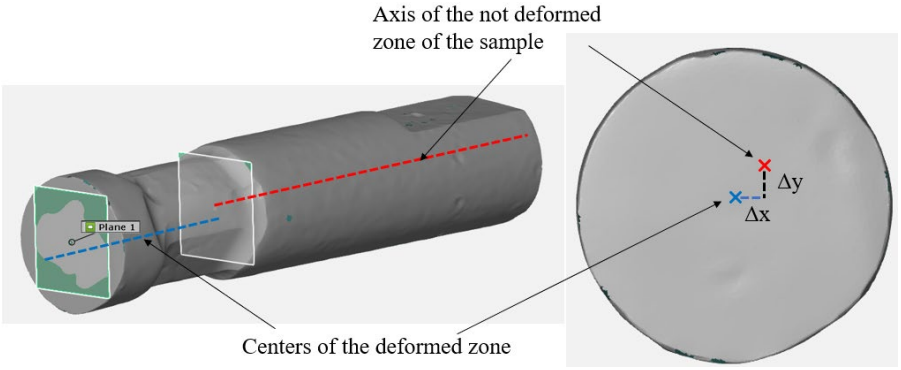

Fig.8 Geometry of an experimentally forged sample and schematic emphasised representation of the bending defect.

On Fig.9, are presented the micrographs of the drilled samples that have undergone the first stroke and first two strokes of the forming route.

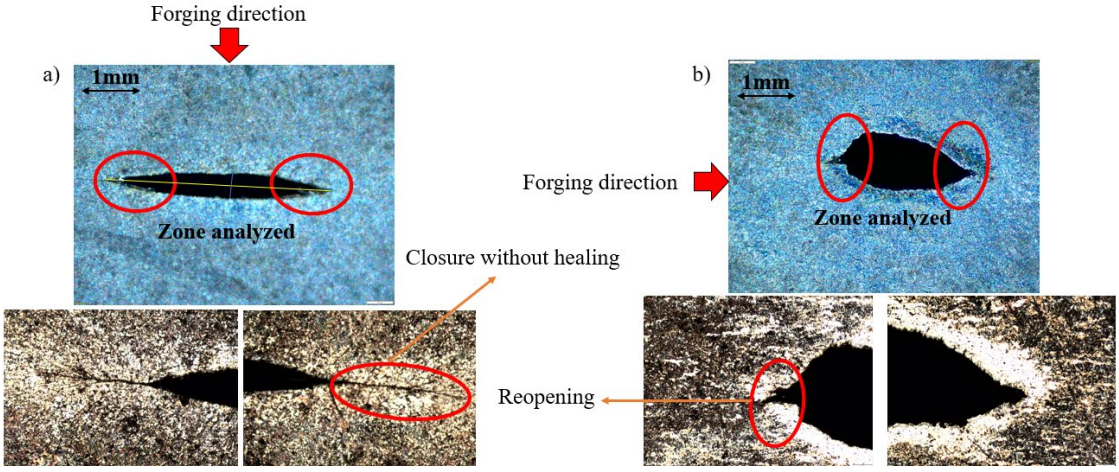

Fig.9 Micrography of the cross section of the drilled sample forged in two stages a) V120 b) V120-V90 with alternations of forging direction.

After the first stroke (V120), the closure was observed. The extremities exhibit contact lines but, because of the presence of an oxide layer, no healing is observed. After the second stroke (V90), mainly due to the alternation of load direction, the reopening of the hole was observed. The

dimensions of the hole were measured from the micrography and are compared with the simulation (see Fig.10).

A cross-section analysis of the simulated geometry of the hole is performed at the center of the deformed zone. The dimensions D1 and D2 are respectively the dimensions of the hole parallel and perpendicularly to the forming direction of the first stroke. The evolution of D1 and D2 and their ratios are plotted according to the equivalent strain along with experimental results as shown in Fig.10. It is observed that for the first stroke (V120) the value of D1 and D2 decreases. The dimension parallel to the forming direction, D1, decreases faster. For the next stroke, because of the alternation of the forging direction, the hole is initially elongated and flat according to a plane containing the new forming direction. This leads to the reopening of the hole.

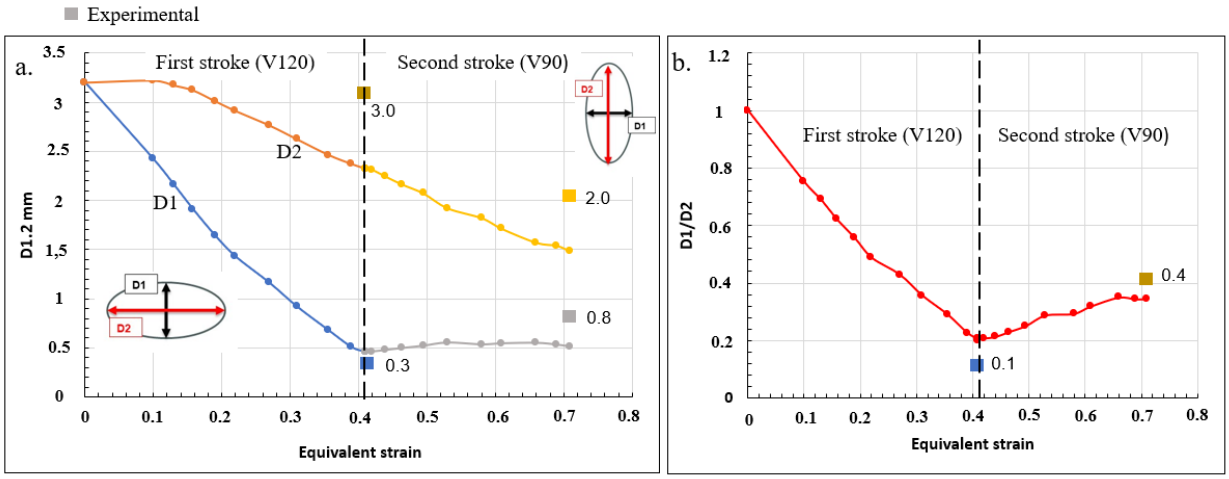

Fig.10 Evolution of geometries of hole with respect to the equivalent strain for two strokes a) D1 and D2 b) D1/D2.

In Fig.10, it can be seen that the void closure is overestimated by the simulation. This can be due to numerical difficulties to simulate the contact line during the closure. The mesh size, the use of the megamaf function or the hole self-contact friction coefficients can be considered in a numerical study to optimize the prediction.

Conclusions

This article presents a set-up for the experimental simulation of void closure under thermomechanical conditions representative of industrial hot rolling. This set-up consists in a succession of free forging strokes applied radially by shaped anvils on a cylindrical sample containing a porosity. The designed set of V-shaped (90° and 120°) and flat anvils allows reproducing the main characteristics of the hot rolling thermomechanical fields with respect to void closure, namely, the equivalent plastic strain, the mean stress triaxiality and the alternation of the forging direction between two successive stages.

One of the main difficulties of the experiment lie in the in-situ measurement of the deformed sample geometry to control the repositioning of the sample between two strokes. To solve partially this problem, the gripper was instrumented, and a laser sensor was implemented so as to measure the total elongation of the sample and to allow the calculation of the actual position of the porosity.

The first experiments performed with drilled samples demonstrated the key influence of the alternation of the forming direction. They also highlighted numerical difficulties to simulate the void closure when the internal contact gets into contact with itself.

The future work will first concern the optimization of the FE simulation of the simulator and especially the simulation of the void closure. The simulator will be applied to samples containing real shrinkage porosities as in Pondaven et al. work [3] with the objective to validate a full-field

model of void closure. A longer-term objective is the use of the validated model in the frame of numerical design of experiments to characterize the influence of the void geometry and tortuosity on its closure during hot rolling.

Acknowledgements
The authors are grateful to Alexandre Fendler for his technical contribution during the experiments. The authors express their thanks to ISEETECH for the provision of the VULCAIN Platform facilities.

References

[1] C. Y. Park et D. Y. Yang, « Modelling of void crushing for large-ingot hot forging », *J. Mater. Process. Technol.*, vol. 67, nº 1-3, p. 195-200, mai 1997. https://doi.org/10.1016/S0924-0136(96)02843-9

[2] M. Saby, « Understanding and modeling of void closure mechanisms in hot metal forming processes ». 2013.

[3] C. Pondaven, L. Langlois, B. Erzar, et R. Bigot, « Numerical and experimental simulation of shrinkage porosity closure during hot rolling of bars », *ESAFORM 2021*, avr. 2021. https://doi.org/10.25518/esaform21.1896

[4] M. Saby, P.-O. Bouchard, et M. Bernacki, « Void closure criteria for hot metal forming: A review », *J. Manuf. Process.*, vol. 19, p. 239-250, août 2015. https://doi.org/10.1016/j.jmapro.2014.05.006

[5] P. Hibbe, M. Wolfgarten, et G. Hirt, « Investigation of void closure in open-die forging considering changing load directions », *Prod. Eng.*, vol. 13, nº 6, p. 703-711, déc. 2019. https://doi.org/10.1007/s11740-019-00924-0

[6] M. Kukuryk, « Experimental and FEM Analysis of Void Closure in the Hot Cogging Process of Tool Steel », *Metals*, vol. 9, nº 5, Art. nº 5, mai 2019. https://doi.org/10.3390/met9050538

[7] G. Banaszek, K. Ozhmegov, A. Kawalek, S. Sawicki, M. Magzhanov, et A. Arbuz, « Investigation of the Influence of Hot Forging Parameters on the Closing Conditions of Internal Metallurgical Defects in Zirconium Alloy Ingots », *Materials*, vol. 16, nº 4, Art. nº 4, janv. 2023. https://doi.org/10.3390/ma16041427

[8] C. Feng et Z. Cui, « A 3-D model for void evolution in viscous materials under large compressive deformation », *Int. J. Plast.*, vol. 74, p. 192-212, nov. 2015. https://doi.org/10.1016/j.ijplas.2015.06.012

[9] C. Pondaven, L. Langlois, R. Bigot, et D. Chevalier, « FEM-Based Methodology for the Design of Reduced Scale Representative Experimental Testing Allowing the Characterization of Defect Evolution during Hot Rolling of Bars », *Metals*, vol. 10, nº 8, Art. nº 8, août 2020. https://doi.org/10.3390/met10081035